JOURNAL OF MATERIALS SCIENCE 21 (1986) 1398–1404

Loss of entanglement density during crazing

CHRIS S. HENKEE*, EDWARD J. KRAMER
Department of Materials Science and Engineering and Materials Science Center, Cornell University, Ithaca, New York 14853, USA

The formation of fibril surface area during craze growth requires a loss of entangled strand density in the fibrils themselves. To demonstrate the decrease in entangled chain density, thin films of polystyrene are bonded to soft copper grids and strained in tension. This procedure produces crazed specimens in which the craze fibrils can be characterized by a well-defined draw ratio, λ_0. The films are then exposed to electron irradiation. This produces chemical crosslinks between the molecules, thus forming a crosslinked network. Subsequent heating of the film above T_g results in the entanglement network trying to retract to $\lambda = 1$. The crosslink network, however, tries to maintain the λ of the craze fibrils at λ_0. The craze fibrils thus retract to Ferry's "state of ease", λ_s, where the tension of the entanglement network is balanced by the compression of the crosslink network. Measurements of λ_s in crazes crosslinked and then healed confirm that a 25 to 50% loss of entanglement density in craze fibrils occurs, in agreement with theoretical predictions.

1. Introduction

An understanding of failure mechanisms in polymer glasses is necessary for rational design with existing polymers and for guidance in modifying such polymers to improve their engineering properties. Often, particular failure characteristics can be related to the associated plastic deformation that occurs prior to loss of mechanical integrity. For example, crack nucleation in many brittle polymer glasses takes place inside crazes where there is a highly localized region of large plastic strain.

The predominant feature that distinguishes crazes from other types of deformation is the network of fine fibrils (5 to 30 nm in diameter) that span the craze surfaces [1–8]. In uncrosslinked polystyrene (PS), the fibrils represent polymer material that has been drawn out to an extension ratio of $\lambda_0 \simeq 4$ [9]. Macroscopic fracture is thought to occur when some of the fibrils break down after long times or under large applied loads to form a void several fibrils in diameter; this void can grow via adjacent fibril breakdown until a sub-critical crack is formed. Finally, as adjacent fibril breakdown continues, the crack reaches critical size and fast fracture ensues.

Another common deformation mode that is often observed in addition to, or instead of, crazing is that of shear deformation [10–18]. This type of deformation is observed upon tensile deformation of thin sheets or films as plane stress deformation zones (DZs) [19–23]. DZs are similar to crazes in that they represent polymer that has undergone elongation in a very localized region. However, unlike crazes, DZs have no well-defined fibril structure, but exhibit a homogeneous strain or extension ratio over the region of deformation. The draw ratios in DZs are also typically lower ($\lambda_0 < 2$) than those of crazes ($\lambda_0 > 2$) [24–26].

Recent experimental observations on the plastic deformation behaviour of various glassy thermoplastics [24–28] can be understood in terms of the entanglement network formed by the polymer molecules [29–31]. The density of network chains, ν_e, between localized points of entanglement can be used to characterize such a network. We are well aware that such a model cannot fully describe the viscoelastic properties of the melt (the tube models, for example, seem superior in that case) [32–35]. Nevertheless, to describe deformation properties in the glassy state, in which reptation times must be long, the network model may still be appropriate. The entanglement density is given by

$$\nu_e = N_A \varrho / M_e \quad (1)$$

where ϱ is the density of the polymer, N_A is Avagadro's number and M_e is the entanglement molecular weight as determined from measurements of the shear modulus of the melt in the rubbery plateau region just above the glass transition temperature, T_g.

The creation of the void–fibril structure of a craze in such a network of entangled chains requires fundamental changes in the network during craze nucleation and growth. Specifically, the creation of (fibril) surface area within a network must involve either (i) scission of some of the network strands or (ii) a certain degree of disentanglement. Regardless of which mechanism dominates, the outcome of either process leads to an entanglement density, ν_e', in the craze fibrils that is lower than that, ν_e, in the bulk amorphous polymer.

Note that in the case of DZ formation, since no new surface area is produced internally, it is not necessary to have any associated entanglement loss. (This predicted loss of entanglement density in crazes, which does not occur for DZs, has been suggested as one

* *Present Address*: Mobil Chemical Company, Central Research, PO Box 240, Edison, NJ 08818, USA.

0022–2461/86 $03.00 + .12

reason for the generally higher draw ratios observed in crazes.) Although quantitative estimates of the degree of entanglement loss that must accompany crazing have been made [36–38], there has been only indirect evidence for this entanglement loss to date [26].

In this paper, we describe a method in which Ferry's two-network model for crosslinks and trapped entanglements [39] is applied to the micromechanical properties of crazes, allowing quantitative information regarding the entanglement loss that accompanies craze growth in PS to be obtained. Since the draw ratio of the polymer in the craze fibrils is $\lambda_0 \simeq 4$, the entanglement network can be envisioned as not only having undergone a certain degree of entanglement loss, but the entire network having undergone elongation as well. The sample is then subsequently crosslinked, in effect introducing a crosslinked network of strand density ν_x. These crosslinks between polymer molecules serve to "trap" a certain fraction of the entanglements present. (The probability of an entanglement being trapped is taken to depend on the number of crosslinks per molecule following Langley [40].) The "trapped" entanglements are topologically constrained so that disentanglement is not possible.

Upon heating the sample to above T_g, the elongated entanglement network wants to contract to $\lambda = 1$ and "heal out" the craze. On the other hand, since the crosslinked network was introduced in the state of deformation, it wants to maintain the draw ratio of $\lambda_0 = 4$. Thus, the sample relaxes to some "state of ease", λ_s, where the tension of the trapped entanglement network balances the compression of the crosslinked network.

Ferry used this two-network approach to explain the results obtained in a series of experiments performed on rubbers crosslinked in states of strain [41–48]. Ferry's results revealed that the elasticity of the crosslinked network could be described by Gaussian elasticity theory. Thus, the true stress associated with the crosslinked network, σ_x, in uniaxial deformation would be described [49] by

$$\sigma_x = \frac{E}{3}(\lambda^2 - \lambda^{-1}) \tag{2}$$

where E is Young's modulus. On the other hand, to describe the behaviour of the trapped entanglement network, the Mooney–Rivlin formulation [50, 50] was required. Thus, the true stress associated with the entanglement network, σ_e, would be described by

$$\sigma_e = 2(C_{1n} + C_{2n}\lambda^{-1})(\lambda^2 - \lambda^{-1}) \tag{3}$$

where C_{1n} and C_{2n} are experimentally determined coefficients.

Using these descriptions of the two networks, it was found that the draw ratio in the state of ease, λ_s, could be related to the trapped entanglement strand density ν_t and the ratio λ_0 at which the crosslinked strand density ν_x was introduced by

$$\frac{\nu_x}{\nu_t} = \frac{\lambda_0^2(\lambda_s^3 - 1)[\psi_n + (1 - \psi_n)\lambda_s]}{(\lambda_0^3 - \lambda_s^3)\lambda_s} \tag{4}$$

where ψ_n represents the importance of the Mooney–Rivlin C_{2n} parameters in the entanglement network, i.e.

$$\psi_n = \frac{C_{2n}}{C_{1n} + C_{2n}} \tag{5}$$

The significance of ψ_n in Equation 4 is apparently related to the extent of relaxation that has taken place in the entanglement network before the crosslinks were introduced. Ferry and his co-workers found that for 1, 2-polybutadiene that had been strained and crosslinked near T_g, ψ_n varied from 0.50 if there was negligible relaxation in the entanglement network, and up to 0.89 if significant relaxation was permitted before crosslinking. Kramer [52] has also discussed the application of such a two-network model to rubbers crosslinked and tested in various states of stain.

In the application of this two-network model to a crazed and then crosslinked sample, the value of the draw ratio inside the craze can be used for λ_0 in Equation 4. If the crosslink density ν_x is known, and the state of ease is measured after annealing above T_g, Equation 4 allows the trapped entanglement density ν_t present in the crazes to be extracted. Finally, Langley's relationship allows the total entanglement density ν_e' that was present in the craze to be determined.

2. Experimental procedure

Monodisperse PS with a weight-average molecular weight of $M_w = 390\,000$ and $\bar{M}_w/\bar{M}_n < 1.10$ was dissolved in toluene. Thin films of PS ($\simeq 0.9\,\mu$m thick) were produced by drawing a glass slide from the solution at a constant rate. Since the surface tension of the films themselves could easily obscure the relaxation properties of the craze upon annealing such thin films, it was necessary to nucleate and grow a few very wide crazes. Since dust particles that have been incorporated into the films act as stress concentrators, and hence generally provide the sites for craze nucleation, precautions were taken to ensure that as little dust as possible was introduced into the solutions before films were drawn. These precautions included microfiltering the polymer solution as well as thoroughly pre-cleaning the glass slides.

After drying, a film could be floated off the glass slide on to the surface of a water bath. It could then be picked up on an annealed copper grid, the bars of which had previously been coated with a film of the same polymer solution. Bonding of the film to the grid was achieved by a short exposure to toluene vapour.

After drying, the specimens were mounted in a strain frame and strained in tension. To obtain the required few but wide crazes, the samples were strained at approximately 0.17% h^{-1}. Using such slow rates, it was possible to obtain overall strains in the films of 5 to 10% without significant craze breakdown. (Subsequent transmission electron microscopy (TEM) of such films revealed that crazes up to 4 μm wide could be grown.) The copper grid deforms plastically in the procedure, so that the strain in the polymer film is maintained even when the grid is removed from the strain frame.

These crazed samples were then crosslinked by exposing them to electron irradiation using a Jeol 733 electron microprobe. The specimens were irradiated

using a beam current of 1×10^{-7} A and an accelerating voltage of 40 kV. The electron beam was defocused to a diameter of 0.4 mm and rastered across the sample to expose an area of 8.1 mm^2. Each scan had 1000 lines and each line required 0.5 msec to complete.

Crosslink densities were determined by measuring the gel point of PS under identical microprobe conditions. Such a procedure, which has been described previously [26], allows one to determine the crosslinking rate in the sample. Thus, from the measurement of the crosslinking rate the density of crosslinked strands, ν_x, can be found for any irradiation time.

The crosslinking rate has been observed to depend on the degree of orientation in some polymers [53–55]. To investigate the dependence of the crosslinking rate in oriented PS, careful gel-point measurements were performed on films that were oriented in the hot melt ($\lambda = 2$). While a small decrease in the gel-point dose was observed, the corresponding change in crosslinking rate was less than the uncertainty in the crosslinking rate for the unoriented films.

After the crazed samples had been crosslinked and aged for 48 h, they were heated to 127° C for 15 min to allow retraction to the state of ease. The state of ease attained using this procedure represents the equilibrium value since annealing samples for 1 min, 15 min or 3 h yielded identical results provided that the crosslink density introduced was the same. The heating rate (100 or 0.5° min^{-1}) also made no difference to the draw ratio observed in the state of ease. The state of ease could be obtained by holding the grids over toluene vapour at room temperature, which plasticized the crosslinked films. After annealing, grid squares of interest were cut from the copper grid for analysis by TEM using a Jeol 200CX microscope operating at 200 kV.

To characterize the local extension ratio in a region of deformation, the method developed by Lauterwasser and Kramer [9] and Brown [56] may be used. In a region of localized deformation, the volume fraction of polymer material, v_f, is found from values of the optical densities of the deformed region (ϕ_c), the film (ϕ_f), and a hole through the film (ϕ_h) determined from densitometry of the electron image plate. The value of v_f is then given by

$$v_f = 1 - \left[\frac{\ln(\phi_c/\phi_f)}{\ln(\phi_h/\phi_f)}\right] \quad (6)$$

Since, the plastic deformation processes occur at constant polymer volume, the extension ratio λ of a region is related to v_f by

$$\lambda = 1/v_f \quad (7)$$

In a second set of experiments, PS films were crosslinked ($\nu_x^0 = 3.7 \times 10^{25}$ chains m^{-3}) prior to straining. This process results in DZs as well as crazes forming upon tensile deformation. Thus, when these samples are subsequently crosslinked, annealed and analysed, they provide a direct comparison of the differences in entanglement network modification that takes place between crazes and DZs.

3. Results

A TEM micrograph of a typical craze in PS is shown in Fig. 1a. The craze–bulk interface is abrupt, with well-formed fibrils spanning the craze width. A microdensitometer trace which traverses across the width of the TEM micrograph displayed in Fig. 1a is shown in Fig. 1b.

If a craze such as that shown in Fig. 1a is crosslinked to a crosslink density of $\nu_x = 4.5 \times 10^{25}$ stands m^{-3} and then subsequently annealed, it will lose its well-defined microstructure and relax to the state of ease in which its microstructure is that shown in Fig. 2a. During the early stages of relaxation, the fibrils coalesce into a film. (Observation of crazes after crosslinking but before annealing reveals microstructures virtually identical to that displayed in Fig. 1a; thus, the crosslinking itself does not appear to affect either craze morphology or draw ratio.)

As shown in Fig. 2b, the microdensitometer trace across the width of the annealed craze clearly indicates that the craze–bulk interface is no longer well-defined and a general "smoothing out" of λ is observed to take place. This loss of abruptness at the "craze"–bulk interface is due to the effect of the surface tension of the film itself. Thus, to obtain accurate measurements of λ_s, only crazes of sufficient width that result in well-defined state-of-ease "plateaux" upon annealing were used. In general, the craze must be wider than the film thickness to obtain this condition.

Table I shows the different state-of-ease draw ratios measured for various crosslink densities introduced into the crazed PS films. It is clear that there is an increase in λ_s as the crosslink density is increased.

Upon tensile deformation of the samples that had been crosslinked prior to straining, DZs were observed to form in association with crazes as shown in Fig. 3a. Generally, the region of deformation contained a fibrillated craze structure at its centre, with DZs forming at the craze "tips". The draw ratio in the crazed region was typically $\lambda_0 \simeq 2.4$, whereas the DZs at the craze tips were found to have $\lambda_0 \simeq 1.7$.

When these samples were crosslinked and then annealed, it was evident which regions originally were the crazed areas, and which regions were the DZs. A TEM micrograph displaying the typical annealed microstructure is shown in Fig. 3b. In these samples, a draw-ratio "plateau" was difficult to ascertain in both the annealed and the unannealed samples. However, the high crosslink densities and the low draw ratios resulted in little variation among specimens that

TABLE I The state of ease, λ_s, measured in annealed crazes as a function of the crosslink density, ν_x, introduced before annealing

ν_x ($\times 10^{25}$ m^{-3})	λ_s
2.0	1.58
3.2	1.97
5.4	2.14
7.3	2.31
12.6	3.05
18.2	2.82
21.8	3.61
Unannealed	$\lambda_0 = 4.16$

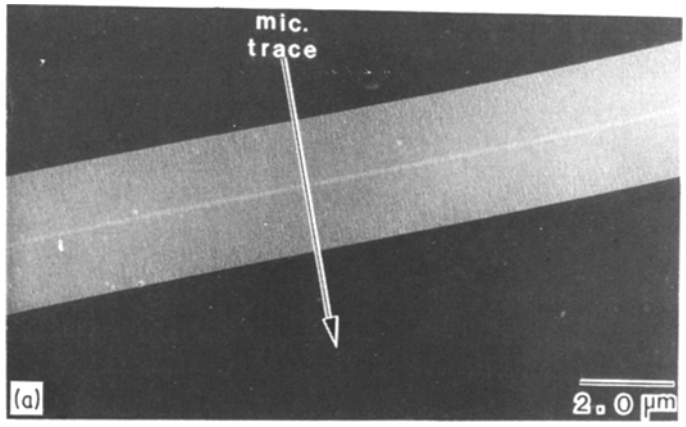

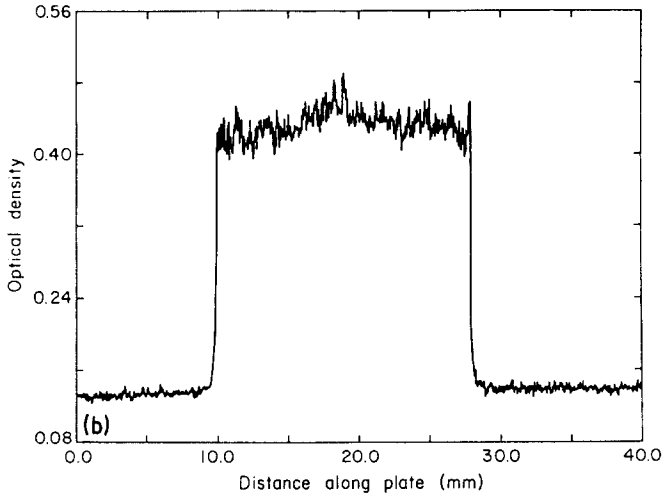

Figure 1 (a) TEM craze micrograph of a typical craze in PS. (b) A microdensitometer trace across the craze micrograph shown in (a) as indicated.

had been irradiated to the same value of ν_x. By using a number of samples prepared identically, it was therefore possible to obtain a consistent value for λ_s at any given crosslink density for both the crazes and DZs.

The resulting measurements of λ_s in the hybrid craze–DZ structures are shown in Table II as a function of the crosslink density introduced in the strained state prior to annealing. As was observed in the previous samples, when the crosslink density is increased, the elongated regions maintain a greater percentage of their deformation upon annealing.

4. Discussion

Turning first to the DZ regions of the hybrid craze–DZ structures, it must be realized that the behaviour predicted by Equation 4 should not be applicable to DZs since the process of DZ growth and the relaxation is not uniaxial in nature. The DZ is only free to contract or expand in a direction normal to the film thickness; it is constrained from deforming along a direction in the plane of the film which is parallel to the DZ edges or shoulders. With this constraint, it is found that the state of ease for DZs should fulfill the conditions [57–59]

$$\frac{\nu_x}{\nu_t} = \frac{(\lambda_s^4 - 1)\,\lambda_0^2}{\lambda_0^4 - \lambda_s^4} \tag{8}$$

It must also be realized that for the case of both crazes and DZs, the behaviour predicted by Equations 4 and 8 must be corrected to account for the effect of the surface tension of the bulk films. This correlation can be shown to be an important consideration by calculating a typical rubber-elastic force being exerted by the crosslink network in the state of ease. For a DZ with $\lambda_0 = 1.67$ and $\lambda_s = 1.3$, with $\nu_x = 7.24 \times 10^{25}$ chains m^{-3}, then at 393 K an effective force per unit length, $f_x \simeq 0.31\,N\,m^{-1}$ will act on the DZ cross-section of a film whose original thickness is one micrometre.

By comparison, the surface tension of both of the PS surfaces will exert an effective force of $\sim 0.066\,N\,m^{-1}$. This calculation reveals that surface tension can be an appreciable fraction of the forces that govern the ultimate draw ratio in the state of ease. Since surface tension will aid the recovery of the DZ, the surface tension force may be added to the forces due to the entanglement contribution of the composite network to determine a corrected value of λ_s.

TABLE II The state of ease, λ_s, measured in annealed hybrid craze–DZ structures such as that shown in Fig. 3; ν_x is the crosslink density that was introduced before annealing

ν_x ($\times 10^{25}$ m^{-3})	λ_s	
	Craze	DZ
7.8	1.66	1.28
10.3	1.75	1.38
15.6	2.18	1.43
20.8	2.03	1.47
24.3	2.08	1.53
Unannealed	$\lambda_0 = 2.33$	1.67

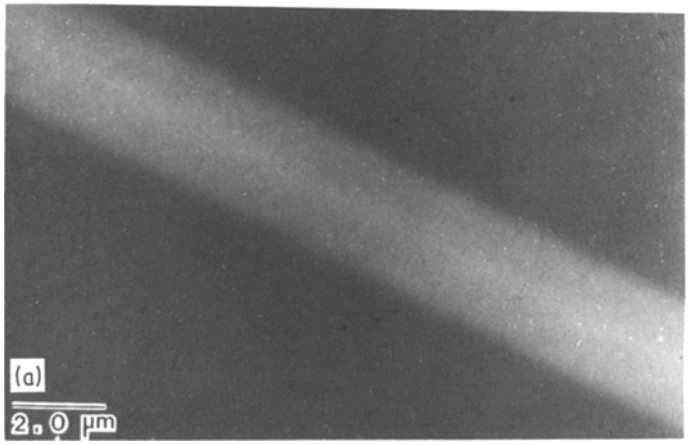

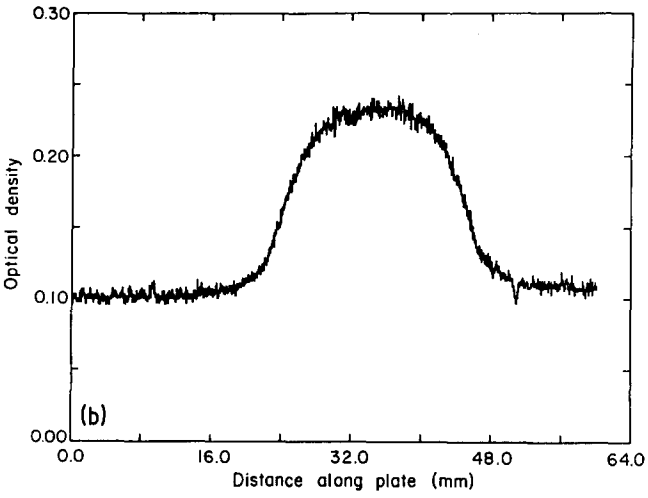

Figure 2 (a) TEM micrograph of a craze like that shown in Fig. 1a, after crosslinking to $\nu_x = 4.5 \times 10^{25}$ chains m^{-3} and annealing above T_g.

At the levels of crosslink density introduced into these samples, well over 90% of the entanglements in the DZs will be trapped. Since little or no chain scission is expected to be associated with the growth of DZs, ν_x/ν_t may be calculated by taking ν_x to be the crosslink density introduced after deformation; ν_t can be taken to be equal to $(\nu_e + \nu_x^0)$ where ν_x^0 is the crosslinked density introduced before deformation. Thus, the behaviour predicted by Equation 8 (after correction for surface-tension effects) can be calculated and compared with the experimental results as shown in Fig. 4. As revealed by the plot in Fig. 4, the agreement of the experimental measurements of λ_s with the behaviour predicted by the two-network model is reasonable.

A plot of λ_s against ν_x for the crazed portion of the hybrid craze–DZ regions is shown in Fig. 5. The behaviour of λ_s as predicted by Equation 4 (after correction for surface-tension effects) is also shown for comparison. No entanglement loss is assumed for this illustration. Since the deformation and crosslinking occurred in the glass, it is expected that little or no molecular relaxation took place in the network before the crosslinks were introduced.

The value of ψ_n is thus taken to be $\psi_n = 0.50$, the value which Ferry [39] found valid for the case in

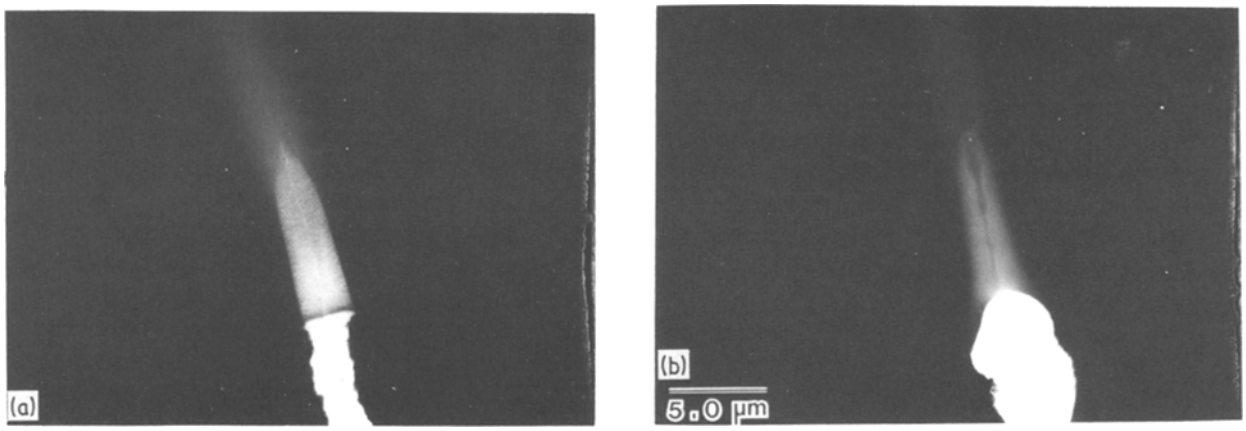

Figure 3 (a) Region of local deformation that was observed to form in response to deformation of PS that had been crosslinked to $\nu_x^0 = 3.7 \times 10^{25}$ chains m^{-3}. (b) Region such as that shown in (a) that had been crosslinked with an additional $\nu_x = 7 \times 10^{25}$ strands m^{-3} and then annealed above T_g.

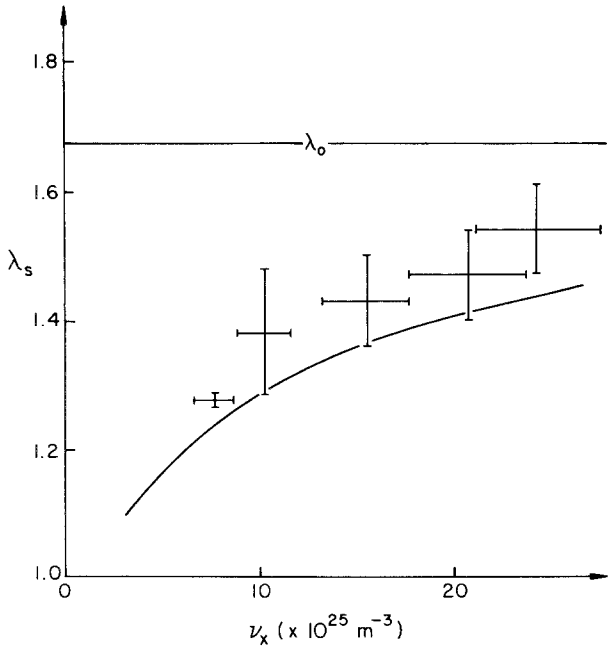

Figure 4 The state of ease, λ_s, measured in annealed DZ regions of hybrid craze–DZ structures such as that shown in Fig. 3. ν_x is the crosslink density that was introduced before annealing but after deformation. The predicted behaviour is also indicated.

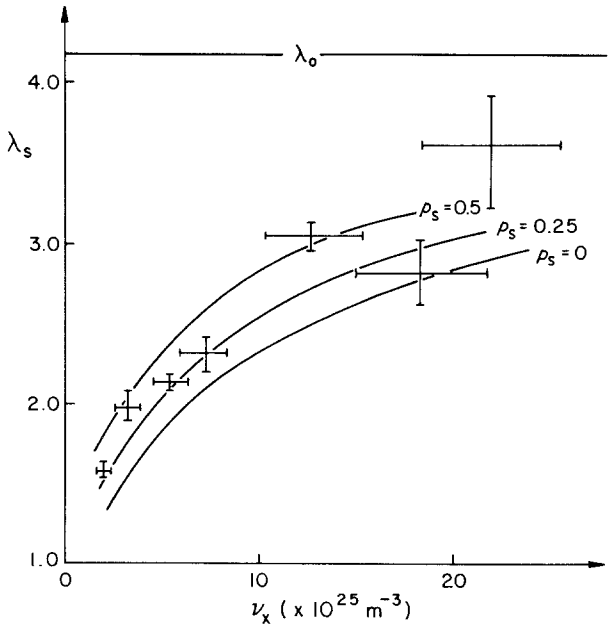

Figure 6 The state of ease, λ_s, measured in annealed crazes in initially uncrosslinked PS as a function of the crosslink density introduced before annealing but after deformation. The lines show the predicted behaviour for several different entanglement loss fractions, p_s.

which essentially no relaxation took place in his experiments on 1,2-polybutadiene (PB). Although ψ_n might be expected to vary slightly between crosslinked networks of PS and PB, this variation should be small compared to the changes in ψ_n expected if different amounts of molecular relaxation have been allowed to take place before crosslinking. In addition, the experimental error in λ_s makes small variations in ψ_n unimportant.

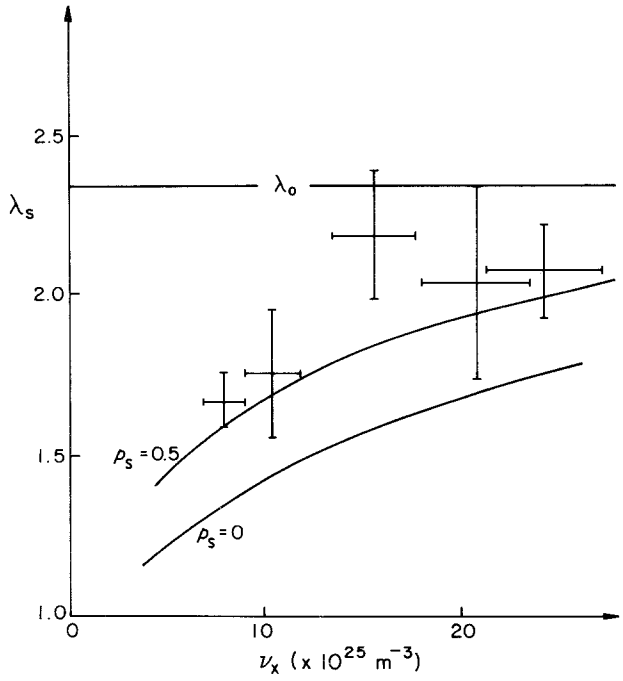

Figure 5 The state of ease, λ_s, measured in annealed craze regions of hybrid craze–DZ structures such as those shown in Fig. 3. ν_x is the crosslink density that was introduced before annealing but after deformation. The expected behaviour for the cases of no entanglement density loss (p_s = 0) and a 50% entanglement density loss (p_s = 0.5) are also shown.

The comparison shown in Fig. 5 reveals that measured values of λ_s are significantly higher than those predicted by the two-network model for no entanglement loss, $\nu_e' = \nu_e$. The disagreement between the predicted and measured values of λ_s in crazes can be understood if a certain loss of entanglement density occurs upon fibrillation. For example, a plot of Equation 4 (corrected for surface-tension effects) is also shown for which $p_s = \nu_e'/\nu_e$ taken to be 0.5. From Fig. 5, there is evidence for a loss of entanglement stand density of nearly 50% during the growth of the fibrillated regions.

Finally, the results for crazes grown in uncrosslinked PS are shown in Fig. 6. Again, the behaviour predicted by the two-network model (corrected for surface tension) falls below the measured values if no entanglement loss is taken into account. By fitting the predicted behaviour to the experimental values, there is evidence for a strand density loss of approximately 25%. The value of entanglement loss predicted from the model of necessary entanglement loss [37, 38] is 60%. The higher values of p_s predicted from the model of necessary entanglement loss may be due in part to the assumption in the model of perfectly cylindrical fibrils that are not connected by cross-tie fibrils. The important point is that a significant loss of entanglement density due to craze fibrillation has been observed.

5. Conclusions

1. Measurements of the state of ease in thin films of polymers deformed in the glassy state and then crosslinked by electron irradiation can yield useful information on changes in a molecular network produced by deformation.

2. Applying this technique to crazes in polystyrene results in the conclusion that 25 to 50% of these

network strands are lost during fibrillation. In the case of crosslinked polystyrene, this loss must be by chain scission.

3. Little or no network strand loss is observed in shear deformation zones in polystyrene.

Acknowledgements

The financial support of this work by the National Science Foundation through the Cornell Materials Science Center is gratefully acknowledged. We thank Professor J. D. Ferry for stimulating correspondence on the two-network model.

References

1. P. BEAHAN, M. BEVIS and D. HULL, *Phil. Mag.* **24** (1971) 1267.
2. S. RABINOWITZ and P. BEARDMORE, *CRC Revs. Macromol. Sci.* **1** (1972) 1.
3. R. P. KAMBOUR, *J. Polym. Sci. Macromol. Rev.* **7** (1973) 1.
4. T. E. BRADY and G. S. Y. YEH, *J. Mater. Sci.* **8** (1973) 1083.
5. P. BEAHAN, M. BEVIS and D. HULL, *ibid.* **8** (1974) 162.
6. S. T. WELLINGHOFF and E. BAER, *J. Macromol. Sci.* **B11** (1975) 367.
7. P. BEAHAN, M. BEVIS and D. HULL, *Proc. R. Soc.* **A343** (1975) 525.
8. D. L. G. LAINCHBURY and M. BEVIS, *J. Mater. Sci.* **11** (1976) 222.
9. B. D. LAUTERWASSER and E. J. KRAMER, *Phil. Mag.* **39A** (1979) 469.
10. A. S. ARGON, R. D. ANDREWS, J. A. GODRICK and W. WITNEY, *J. Appl. Phys.* **39** (1968) 1899.
11. P. B. BOWDEN and S. RAHA, *Phil. Mag.* **22** (1970) 463.
12. E. J. KRAMER, *J. Macromol. Sci.* **B10** (1974) 191.
13. G. A. ADAM, A. CROSS and R. N. HAWARD, *J. Mater. Sci.* **10** (1975) 1582.
14. J. B. C. WU and J. C. M. LI, *ibid.* **11** (1976) 434.
15. *Idem, ibid.* **11** (1976) 445.
16. S. T. WELLINGHOFF and E. BAER, *J. Appl. Polym. Sci.* **22** (1978) 2025.
17. C. C. CHAU and J. C. M. LI, *J. Mater. Sci.* **14** (1979) 1593.
18. *Idem, ibid.* **14** (1979) 2172.
19. N. J. MILLS, *Eng. Frac. Mech.* **6** (1974) 537.
20. I. NARISAWA, M. ISHIKAWA and H. OGAWA, *Polymer J.* **8** (1976) 181.
21. M. ISHIKAWA, I. NARISAWA and H. OGAWA, *ibid.* **8** (1976) 391.
22. A. M. DONALD and E. J. KRAMER, *J. Mater. Sci.* **16** (1981) 2967.
23. *Idem, ibid.* **16** (1981) 2977.
24. *Idem,* **23** (1982) 1183.
25. *Idem, J. Polym. Sci., Polym. Phys. Ed.* **20** (1982) 899.
26. C. S. HENKEE and E. J. KRAMER, *ibid.* **22** (1984) 721.
27. A. M. DONALD, E. J. KRAMER and R. A. BUBECK, *ibid.* **20** (1982) 1129.
28. A. M. DONALD and E. J. KRAMER, *Polymer* **23** (1982) 461.
29. J. D. FERRY, in "Viscoelastic Properties of Polymers", 3rd Edn, (Wiley, New York, 1980) p. 366.
30. W. W. GRAESSLEY, *Adv. Polym. Sci.* **16** (1974) 1.
31. S. ONOGI, T. MASUDA and K. KITAGAWA, *Macromol.* **3** (1970) 111.
32. P. D. deGENNES, *J. Chem. Phys.* **55** (1971) 572.
33. M. DOI and S. F. EDWARDS, *J. Chem. Soc., Faraday Trans. 2* **74** (1978) 918.
34. *Idem, ibid.* **74** (1978) 1789.
35. *Idem, ibid.* **74** (1978) 1802.
36. E. J. KRAMER, *Adv. Polym. Sci.* **52/53** (1983) 1.
37. *Idem, Polym. Eng. Sci.* **24** (1984) 761.
38. C. C. KUO, S. L. PHOENIX and E. J. KRAMER, *J. Mater. Sci. Lett.* **4** (1985) 459.
39. J. D. FERRY, *Polymer* **20** (1979) 1343.
40. N. R. LANGLEY, *Macromol.* **1** (1968) 348.
41. O. KRAMER, R. L. CARPENTER, V. TY and J. D. FERRY, *ibid.* **7** (1974) 79.
42. O. KRAMER and J. D. FERRY, *ibid.* **8** (1975) 87.
43. R. L. CARPENTER, O. KRAMER and J. D. FERRY, *ibid.* **10** (1977) 117.
44. *Idem, J. Appl. Polym. Sci.* **22** (1978) 335.
45. R. L. CARPENTER, H. C. KAN and J. D. FERRY, *Polym. Eng. Sci.* **19** (1979) 267.
46. H. C. KAN and J. D. FERRY, *Macromol.* **11** (1978) 1049.
47. H. C. KAN, R. L. CARPENTER and J. D. FERRY, *J. Polym. Sci., Polym. Phys. Ed.* **17** (1979) 1855.
48. H. C. KAN and J. D. FERRY, *Macromol.* **12** (1979) 494.
49. L. R. G. TRELOAR, *Rep. Prog. Phys.* **36** (1973) 755.
50. D. S. PEARSON, B. J. SKUTNIK and G. G. A. BOHM, *J. Polym. Sci., Polym. Phys. Ed.* **12** (1974) 925.
51. J. D. FERRY and H. C. KAN, *Rubber Chem. Technol.* **51** (1978) 731.
52. O. KRAMER, *Polymer* **20** (1979) 1336.
53. D. E. ROBERTS and L. MANDELKERN, *J. Amer. Chem. Soc.* **80** (1958) 1289.
54. R. KITAMARU and L. MANDELKERN, *Polym. Lett.* **2** (1964) 1019.
55. A. CHARLESBY, D. LIBBY and M. G. OMEROD, *Proc. R. Soc.* **A262** (1961) 207.
56. H. R. BROWN, *J. Mater. Sci.* **14** (1979) 237.
57. J. P. BERRY, J. SCANLAN and W. F. WATSON, *Trans. Faraday Soc.* **52** (1956) 1137.
58. A. GREENE, K. J. SMITH and A. CIFERRI, *ibid.* **61** (1965) 2772.
59. C. S. HENKEE, PhD thesis, Cornell University (1985).

Received 8 May
and accepted 12 June 1985